

Electrical Surface Potential of Pulmonary Surfactant

Zoya Leonenko,[†] Mathias Rodenstein,[‡] Jana Döhner,[†] Lukas M. Eng,[‡] and Matthias Amrein^{*,†}

Department of Cell Biology and Anatomy, Faculty of Medicine, University of Calgary, 3330 Hospital Drive NW, T2N 4N1, Alberta, Canada, and Institute of Applied Photophysics, University of Technology Dresden, D-01062 Dresden, Germany

Received June 14, 2006. In Final Form: August 16, 2006

Pulmonary surfactant is a mixed lipid protein substance of defined composition that self-assembles at the air–lung interface into a molecular film and thus reduces the interfacial tension to close to zero. A very low surface tension is required for maintaining the alveolar structure. The pulmonary surfactant film is also the first barrier for airborne particles entering the lung upon breathing. We explored by frequency modulation Kelvin probe force microscopy (FM-KPFM) the structure and local electrical surface potential of bovine lipid extract surfactant (BLES) films. BLES is a clinically used surfactant replacement and here served as a realistic model surfactant system. The films were distinguished by a pattern of molecular monolayer areas, separated by patches of lipid bilayer stacks. The stacks were at positive electrical potential with respect to the surrounding monolayer areas. We propose a particular molecular arrangement of the lipids and proteins in the film to explain the topographic and surface potential maps. We also discuss how this locally variable surface potential may influence the retention of charged or polar airborne particles in the lung.

Introduction

A molecular film of pulmonary surfactant separates the hydrated lung epithelium from the air. Pulmonary surfactant is distinguished by a high proportion of saturated phospholipids, cholesterol and specific surfactant proteins. The film lowers the surface tension of the air–lung interface and thus provides stability to the alveolar structure and reduces the work of breathing. Here we used films formed from bovine lipid extract surfactant (BLES)¹ to investigate the local electrical surface potential in addition to the surface topology using Kelvin probe force microscopy (KPFM). BLES contains all lipids of natural surfactant with the exception of cholesterol, which is removed from this preparation. BLES, like most natural surfactants, contains about 40 wt % dipalmitoylphosphatidylcholine (DPPC), a fully saturated zwitterionic lipid.¹ BLES also contains the two highly hydrophobic surfactant associated proteins B and C. When spread at an air–water interface of a Langmuir trough, BLES undergoes phase separation with domains of likely pure DPPC in a matrix of the more fluid unsaturated lipids and hydrophobic proteins.² In the current study, we used BLES in its original composition and after adding 5% cholesterol (weight) to reflect a natural proportion in the surfactant. Cholesterol at such a proportion has been shown to have a marked effect on the film structure in that it disperses the large DPPC domains.^{3–10}

We evaluated the local surface potential of the pulmonary surfactant film as a means to obtain a more complete picture of its local composition and molecular arrangement. Lipid films at an air–water interface exhibit an electrical surface potential. The surface potential is defined as the difference in electrical potential between the film-covered interface to the air and the aqueous subphase. The potential arises from aligned molecular dipoles (for a review of the surface potential of interfacial films, see ref 11). In the case of the complex structural organization of the phase-separated film of pulmonary surfactant, a map of the local surface potentials promises insight into the local distribution and order of the molecular constituents.

Another reason for studying the surface potential of pulmonary surfactant is its possible interference with charged or polar airborne particles in the breathing air. A surface potential of the surfactant film may define whether the fraction of nanometer-sized airborne particles that enter the deep (alveolar) lung are exhaled or make contact with the alveolar wall and enter the body. Epidemiological studies show consistently that high levels of these particles in the air are associated with substantial respiratory and cardiovascular morbidity and mortality.^{12–14} Such particles, on the other hand, offer an excellent opportunity to administer drugs to the distal lung and, through the bloodstream, to the rest of the body.

Kelvin probe force microscopy (KPFM) is a scanning probe technique which is capable of mapping the local surface potential with spatial resolution in the nanometer range. At the same time as a topographical image of the interface is acquired, as in a conventional atomic force microscope (AFM), the electrostatic interaction between the electrically conductive AFM tip and the

[†] University of Calgary.

[‡] University of Technology Dresden.

(1) Yu, S.; Harding, P. G.; Smith, N.; Possmayer, F. *Lipids* **1983**, *18* (8), 522–529.

(2) Nag, K.; Perez-Gil, J.; Ruano, M. L.; Worthman, L. A.; Stewart, J.; Casals, C.; Keough, K. M. *Biophys. J.* **1998**, *74* (6), 2983–2395.

(3) de la Serna, J. B.; Perez-Gil, J.; Simonsen, A. C.; Bagatolli, L. A. *J. Biol. Chem.* **2004**, *279* (39), 40715–40722.

(4) Diemel, R. V.; Snel, M. M. E.; van Golde, L. M. G.; Putz, G.; Haagsman, H. P.; Batenburg, J. J. *Biochemistry* **2002**, *41* (50), 15007–15016.

(5) Discher, B. M.; Maloney, K. M.; Grainger, D. W.; Hall, S. B. *Biophys. Chem.* **2002**, *101–102*, 333–345.

(6) Malcharek, S.; Hinz, A.; Hilterhaus, L.; Galla, H. J. *Biophys. J.* **2005**, *88* (4), 2638–2649.

(7) Panda, A. K.; Hune, A.; Nag, K.; Harbottle, R. R.; Petersen, N. O. *Indian J. Biochem. Biophys.* **2003**, *40* (2), 114–121.

(8) Taneva, S. G.; Keough, K. M. W. *Biochemistry* **1997**, *36* (4), 912–922.

(9) Worthman, L. A.; Nag, K.; Davis, P. J.; Keough, K. M. *Biophys. J.* **1997**, *72* (6), 2569–2580.

(10) Yan, C.; Johnston, L. J. *Microsc.* **2002**, *205*, 136–146.

(11) Dynarowicz-Latka, P.; Dhanabalan, A.; Oliveira, O. N., Jr. *Adv. Colloid Interface Sci.* **2001**, *91* (2), 221–293.

(12) Johnston, C. J.; Finkelstein, J. N.; Mercer, P.; Corson, N.; Gelein, R.; Oberdorster, G. *Toxicol. Appl. Pharmacol.* **2000**, *168* (3), 208–215.

(13) Oberdorster, G. *Int. Arch. Occup. Environ. Health* **2001**, *74* (1), 1–8.

(14) Oberdorster, G.; Gelein, R. M.; Ferin, J.; Weiss, B. *Inhalation Toxicol.* **1995**, *7* (1), 111–124.

interface is sensed. For each point of the scanned area, the electrical potential of the tip is adjusted by means of a feedback loop until the electrostatic interaction between tip and sample has vanished. At this time, the potential at the tip equals the local potential of the sample and is recorded. This method of nullifying the potential between the sample under investigation and the measuring electrode is derived from the long-established Kelvin method to measure the surface potential of Langmuir films over macroscopic areas (e.g., ref 11). To date, KPFM on organic films has been successfully used to study amphiphilic molecules^{15–17} and a biological membrane.¹⁸ KPFM has not been applied to pulmonary surfactant so far.

We used a novel scheme of the KPFM, the frequency modulation technique (FM-KPFM).^{19,20} We have shown earlier that the frequency modulation method is preferable over earlier implementation of the KPFM for most applications. It allows simultaneous recording of topographic and local surface potential images with high resolution and greatly improved sensitivity. FM-KPFM derives a surface potential by measuring the gradient of the electrostatic force rather than the force itself. Unlike earlier implementations of KPFM, FM-KPFM is largely insensitive to the geometry of the tip and thus avoids related artifacts.

Experimental Details

Pulmonary Surfactant Films. Pulmonary surfactant films were formed from BLES. BLES in saline (pH 5–6) with a phospholipid concentration of 27 mg/mL was a kind gift of the manufacturer (BLES Biochemical Inc., London, Ontario). We prepared samples containing 0% and 5% (by weight) cholesterol. Cholesterol was purchased from Sigma Chemicals, St. Louis, MO. To add the desired amount of cholesterol, a solution of 1:1:1 ratio of methanol, chloroform, and BLES by volume was first vortexed and then spun at 100g for 5 min. The methanol/water phase was discarded, the BLES in chloroform was retained, and either no cholesterol or 5% cholesterol (by mass) with respect to phospholipids was added. Each solution was then dried under N₂ and resuspended with buffer (140 mM NaCl, 10 mM Hepes, and 2.5 mM CaCl₂; pH 6.9) to obtain solutions of BLES at a concentration of 27 mg/mL phospholipids, containing no cholesterol or 5% cholesterol. The samples were spread at the air–water (buffer) interface of a Langmuir trough from the concentrated buffer solution. The barrier was then moved, until a surface tension of about 25 mN/m was reached. For imaging, the film was deposited on a mica substrate by means of the Langmuir–Blodgett technique. Freshly cleaved ASTMV-2 quality, scratch-free ruby mica (Asheville-Schoonmaker Mica Co., Newport News, VA) was used. During film transfer, the surface tension was kept constant. After deposition of the sample, the mica was clamped to a conductive metal stud.

Microscopy. Topographical images were collected in air with a NanoWizard AFM, (JPK Instruments AG, Berlin). Noncontact-mode silicon cantilevers NCH-20 from NanoWorld were used with the typical spring constant 21–78 N/m and resonance frequency 260–460 kHz (Figure 1). For the combined KPFM and topographical imaging (Figures 2 and 3), a laboratory-made setup as described by Zerweck¹⁹ and chromium/platinum tips were used.

Results and Discussion

Figure 1 shows an overview of the film topography formed by BLES. Patches of lipid bilayer stacks adhere to a molecular

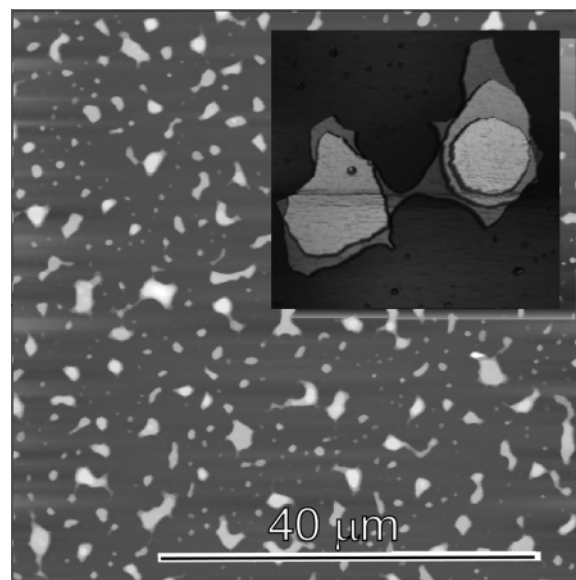


Figure 1. AFM topography of BLES films on mica with 5% cholesterol by weight. The films were formed at the air–water interface of a Langmuir trough and the area reduced until a film pressure of 47 mN/m was reached (corresponding to a surface tension of 26 mN/m). For the microscopy, the films were transferred onto a mica support by the Langmuir–Blodgett technique. Bright patches are stacks of lipid bilayers as indicated by a step height of about 5 nm (see insert, size 2.5 μm by 2.5 μm).

monolayer. This molecular architecture is shared by all functional pulmonary surfactant formulations, able to reduce the surface tension of an air–water interface close to zero.^{21,22} Figure 2 depicts topographical images and corresponding surface potential maps of surfactant films at a higher magnification. The film shown in Figure 2A,B contained no cholesterol, whereas the film in Figure 2C–F contained 5% cholesterol. The film topography reflects the local film thickness. From the equation below, the potential is a function of the strength of the molecular dipoles μ , the dielectric constant ϵ , and the packing density or area A , covered by each molecule A . Only the component of μ in the direction perpendicular to the interface μ_{\perp} contributes to the surface potential (i.e., a dipole arranged parallel to the interface does not). An overview of the methods for characterization of Langmuir monolayers, including the Kelvin method, is available in Dynarowicz-Latka et al.¹¹ For phospholipids, contributions have been ascribed to various regions of the molecules $\mu_{1...3}$, each in its own dielectric environment $\epsilon_{1...3}$: the aqueous layer in proximity of the film, the headgroup region, and the aliphatic tail.^{23,24}

$$V = \frac{1}{A\epsilon_0} \left[\frac{\mu_{\perp 1}}{\epsilon_1} + \frac{\mu_{\perp 2}}{\epsilon_2} + \frac{\mu_{\perp 3}}{\epsilon_3} \right]$$

The equation reveals the importance of the dielectric environment for the contribution of a dipole to the surface potential. If the dipole resides within the aliphatic tail region with an ϵ of about 2,^{23,24} it will contribute much more strongly than a dipole within the hydrated head region with an ϵ close to that of water (80).

In discussing the results, we will first relate the average surface potential of the films to the reported findings for the average

(15) Chi, L. F.; Jacobi, S.; Fuchs, H. *Thin Solid Films* **1996**, 284–285, 403–407.

(16) Jacobi, S.; Chi, L. F.; Fuchs, H. *J. Vac. Sci. Technol., B* **1996**, 14 (2), 1503–1508.

(17) Lu, J.; Delamarche, E.; Eng, L.; Bennewitz, R.; Meyer, E.; Guntherodt, H. *J. Langmuir* **1999**, 15 (23), 8184–8188.

(18) Knapp, H. F.; Mesquida, P.; Stemmer, A. *Surf. Interface Anal.* **2002**, 33 (2), 108–112.

(19) Zerweck, U.; Loppacher, C.; Otto, T.; Grafstrom, S.; Eng, L. *M. Phys. Rev. B* **2005**, 71 (12), 125424–125433.

(20) Loppacher, C.; Zerweck, U.; Teich, S.; Beyreuther, E.; Otto, T.; Grafstrom, S.; Eng, L. *M. Nanotechnology* **2005**, 16 (3), S1–S6.

(21) Lipp, M. M.; Lee, K. Y. C.; Takamoto, D. Y.; Zasadzinski, J. A.; Waring, A. *J. Phys. Rev. Lett.* **1998**, 81 (8), 1650–1653.

(22) Nahmen von, A.; Schenk, M.; Sieber, M.; Amrein, M. *Biophys. J.* **1997**, 72, 463–469.

(23) Vogel, V.; Mobius, D. *J. Colloid Interface Sci.* **1988**, 126 (2), 408–420.

(24) Demchak, R. J.; Fort, J. T. *J. Colloid Interface Sci.* **1974**, 46 (2), 191.

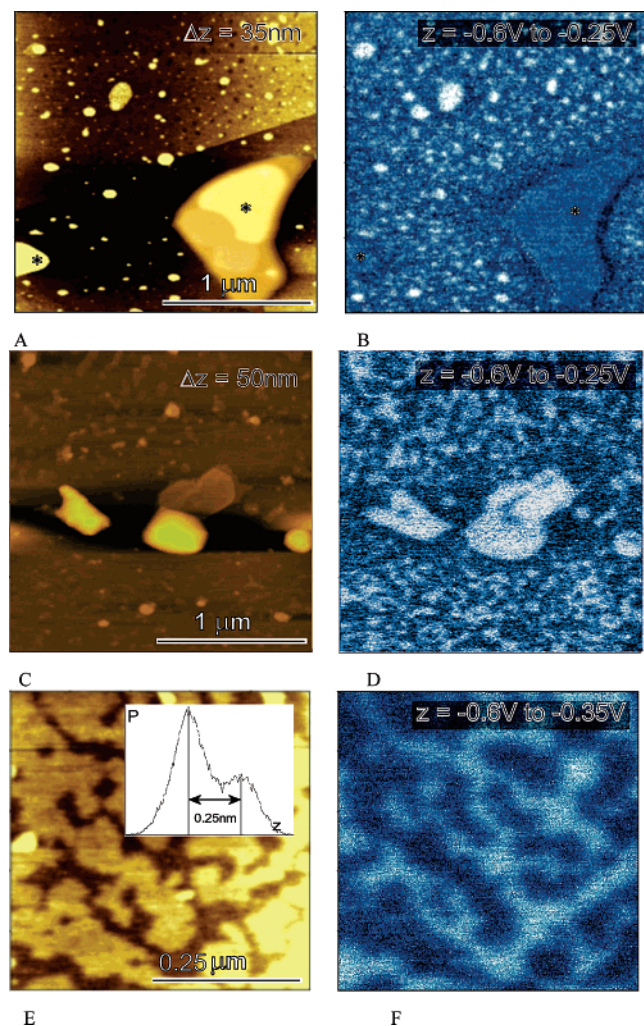


Figure 2. AFM topographies (brown) and surface potential maps (blue) of surfactant films. Top row: BLES + 0% cholesterol, surface tension of 23 mN/m. The small regions of lipid bilayer patches seen in the topography (A) stand out brightly in the potential image (B), indicating a more positive surface potential. However, the two prominent multilayer areas on the bottom left and right of (A) (denoted by *) are not different in the surface potential from the monolayer region. Middle row: BLES + 5% cholesterol (weight), surface tension of 26 mN/m. The lipid bilayer stacks seen in (C) show a more positive surface potential (D), similar to the films containing no cholesterol. However, unlike the films without cholesterol, films containing 5% cholesterol show a structured surface potential also within the monolayer region (F). Surface potential correlates with topographic height, and regions of higher surface potential are about 0.25 nm lower in height (E).

surface potentials obtained by the Kelvin method. Then, a molecular architecture will be proposed to explain the contrast in the potential maps. Finally, we discuss the influence that such a surface potential will have on small, charged airborne particles.

Average Surface Potential. The (dark) monolayer regions in Figure 2 A,C,F are distinguished by a surface potential in the range of -0.6 V (Figure 2B). Because the films in the current study have been transferred onto a mica support, the electrical potential V_{app} is not caused by the surface potential ϕ alone, but is also caused by an additional potential offset between the probe and the mica substrate, V_{CPD} :

$$V_{app} = V_{CPD} + \phi$$

If compared to the reported average surface potential of similar films obtained by the Kelvin method directly at the air–water

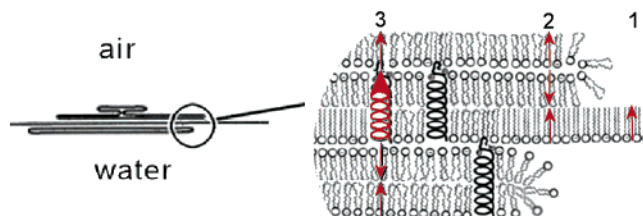


Figure 3. Molecular architecture of pulmonary surfactant. 1, 2, and 3 denote three situations of arrangement of molecular dipoles. The molecular arrangement of pulmonary surfactant films should lead to a positive surface potential in monolayer regions (denoted by 1), a potential similar to that of the monolayer region if a monolayer region is covered by lipid bilayer patches devoid of protein (2), and a region of a more strongly positive surface potential over bilayer patches that contain SP-C (3). The arrows depict the molecular dipole moment, pointing to the positive pole. The dipole of SP-C is depicted with an arrowhead and a helical tail. Note that α -helices are distinguished by a molecular dipole moment in the direction of the helix axis. This is because of the aligned molecular dipole posed by the amide bonds. The dipole sums up to about 1/2 unit charge on each side times the length of the helix.

interface, the offset may be estimated. Films of dipalmitoylphosphatidylcholine (DPPC), the most abundant molecular species in BLES (approximately 40 wt %), have been reported by most authors to give rise to an average surface potential of about +0.5 V at a surface tension of 25 mN/m (the surface tension chosen for the current study).²⁵ V_{CPD} should therefore amount to approximately -1 V. To measure V_{CPD} , KPFM surface potential maps of bare mica support were acquired and revealed a potential of approximately -2 V without any recognizable local variation (results not shown). While this may explain the overall negative surface potential, the potential of mica in the absence of a surfactant film does not likely reflect a good measure of V_{CPD} , because bare mica will always be covered by a water film in an ambient environment and, hence, present a very different interface from that of mica underneath the BLES film. In summary, the KPFM surface potential maps of surfactant showed an offset that could not be exactly determined. To overcome this problem, films may have to be deposited on a conductive support or, even better, investigated by KPFM directly at the air–water interface. Notably, absolute potentials also pose a problem in Kelvin studies directly at the air–water interface. Mozaffary et al.²⁶ reported a negative sign of the surface potential for DPPC, and Oliveira et al.²⁷ found a surface potential for DPPC at a surface tension of 25 mN/m of about 150 mV. Note that, for identical experimental conditions and substrates, one may still compare absolute potentials from one sample to another.²⁸ Most importantly, the offset does not affect the contrast within the potential maps (i.e., the potential difference from one sample location to another).

Contrast in Surface Potential Maps. Segregation of molecular components and the specific molecular arrangement gives rise to the locally variable surface potential (i.e., contrast) seen in Figure 2B,D,F. The most striking feature in the surface potential maps of pulmonary surfactant are the positive (or less negative) regions ($+0.2 \pm 0.05$ V over the background), where in the topography there are stacks of lipid bilayers adjacent to the monolayer. Figure 3 is a schematic explaining the proposed molecular order of the film in relation to the observed contrast in surface potential maps. The potential difference between

(25) Brockman, H. *Chem. Phys. Lipids* **1994**, *73*, 57–79.

(26) Mozaffary, H. *Chem. Phys. Lipids* **1991**, *59*, 39–47.

(27) Oliveira, O. N.; Riul, A.; Leite, V. B. P. *Braz. J. Phys.* **2004**, *34* (1), 73–83.

(28) Lü, J.; Delamar, E.; Eng, L. M.; Bennewitz, R.; Meyer, E.; Güntherodt, H.-J. *Langmuir* **1999**, *15*, 8184–8188.

monolayer and lamellar areas may be explained by the presence of surfactant associated protein C (SP-C) in the latter regions. SP-C is a small (molecular mass ~ 4 kDa) hydrophobic protein with a highly defined lipid bilayer spanning α -helical segment.^{29,30} SP-C possesses a particularly strong molecular dipole moment in the direction of its molecular axis due to the α -helical secondary structure. An α -helix has an overall dipole moment caused by the aggregate effect of all the individual dipoles from the carbonyl groups of the peptide bond pointing along the helix axis. α -Helices are often capped at the N-terminal end by a negatively charged amino acid (or a positively charged C-terminal amino acid) in order to neutralize this helix dipole, but not in SP-C. We have shown that SP-C in the surfactant films promotes the formation of lipid bilayer patches, resides in these multilamellar regions,³¹ and is arranged with its helical axis perpendicular to the interface (discussed in ref 32). If arranged with its N-terminal pointing toward the air, SP-C must therefore effectively induce a more positive surface potential in the multilayered areas of the film (situation 3 in Figure 3) and thus explain the more positive surface potential found on the multilayered regions in Figure 2.

It is notable that the other known hydrophobic surfactant associated protein, SP-B, is also present in BLES and also promotes the formation of lamellar structures.^{33,34} There appear to be five amphipathic helices aligned partially immersed in the lipid layer with the axes parallel to the interface.^{35–37} Since in this case the molecular dipoles of the helices should be mostly parallel to the interface, they should not contribute to the surface potential, according to the equation above.

Interestingly, the sample region depicted in Figure 2A,B also shows two lamellar regions with a surface potential, similar to the surrounding monolayer. These regions may consist of lipid bilayers, devoid of SP-C. Such regions should not show a net contribution to the surface potential as the molecular dipoles from the lower and the upper leaflet of each bilayer are of opposite direction with respect to the sample normal and, as a result, their contributions to the surface potential cancel out (situation 2 in Figure 3). We showed earlier by scanning near-field optical microscopy that multilayered regions with and without SP-C indeed coexist, similar to the situation found here.

Another aspect of the molecular arrangement becomes evident in the monolayer areas of the surfactant films and is different for films with cholesterol as compared to films without. For the film without cholesterol shown in Figure 2A,B, the monolayer areas are structured in neither topography nor the potential map. The contrast in the potential maps strictly follows the pattern of lamellar and monolayer areas. The film with cholesterol shown in Figure 2C–F, on the other hand, shows a contrast of the surface potential (Figure 2D,F) also in the monolayer region alone, and the potential varies by about 0.25 V. The contrast of the potential follows a subtle topographical structure (Figure 2E), with areas 0.25 nm lower (of lesser film thickness) being

distinguished by a higher surface potential. Apparently, here, the molecular components in the monolayer have segregated into small domains of different surface potentials. It is notable that in a light microscope such small domains could not be resolved, which is why cholesterol-containing films appear homogeneous in these microscopes.^{5,7} An understanding of the nature of the small domains observed in both the topography and the potential map may be derived from analogy with the sphingolipid–cholesterol rafts of the plasma membrane. These condensed rafts within the fluid membrane matrix consist of the saturated lipid species of the plasma membrane and cholesterol and have been estimated to be of similar dimensions (approximately 50 nm in diameter) as the domains observed here.^{38,39}

Role of the Surface Potential. The surface potential itself may play a role in defining the molecular architecture of pulmonary surfactant. Formation and size of domains in interfacial films of surfactants are governed by the tension of the line separating domains from a surrounding matrix on one hand and the stress caused by an electrical surface potential within a single domain on the other hand (e.g., ref 40). A high surface potential favors small and dispersed domains, while a high line tension promotes formation of large domains. Cholesterol in mixed films of phospholipids is known to reduce the line tension between domains.^{5,41} The absence of a high line tension in the presence of a surface potential may therefore explain the formation of the small domains seen in Figure 2E,F.

Another important role of the surface potential relates to the interaction of airborne particles entering the lung. Both manmade and natural particles are invariably electrically charged, and their fate in the lung is also influenced by this electrical charge.⁴² The movement of small particles ($<0.5 \mu\text{m}$) in the lung has largely been described to be by diffusion⁴³ and chaotic mixing.^{44,45} However, these small particles will also be affected strongly by electrostatic interaction with the alveolar wall. Bailey et al. have shown that moderately charged particles ($q = 200$ electrons) with a diameter of $0.5 \mu\text{m}$ are deposited in the alveolar lung about 5 times more efficiently than uncharged particles. Until now, any electrostatic interaction of particles with the alveolar wall has been ascribed to the attraction of an electrically charged particle and its electrical image induced in the alveolar wall. We now offer an additional mechanism for this behavior: the interaction of the charged particles with the electrical field arising from the surface potential of the surfactant film.

With respect to its interaction with charged particles, surfactant at the air–water interface might be described as a thin, charged insulator plate (the lipid film) with a conductive backing (the water phase). For an evenly charged film, a marked electrostatic force on a charged aerosol may only be expected after the particle has come into close proximity of the interface, on the order of the film thickness. Otherwise, the electrical potential will drop inside the surfactant film from its air side to the water phase and no electrical field will be present in the air above the film. However, for a structured surface potential such as found in the

(29) Johansson, J.; Szyperski, T.; Curstedt, T.; Wüthrich, K. *Biochemistry* **1994**, *33*, 6015–6023.

(30) Johansson, J.; Szyperski, T.; Wüthrich, K. *FEBS Lett.* **1995**, *362*, 261–265.

(31) Kramer, A.; Wintergalen, A.; Sieber, M.; Galla, H. J.; Amrein, M.; Guckenberger, R. *Biophys. J.* **2000**, *78* (1), 458–465.

(32) Amrein, M.; von Nahmen, A.; Sieber, M. *Eur. Biophys. J.* **1997**, *26* (5), 349–357.

(33) Lipp, M. M.; Lee, K. Y.; Zasadzinski, J. A.; Waring, A. J. *Science* **1996**, *273* (5279), 1196–1199.

(34) Krol, S.; Ross, M.; Sieber, M.; Kunneke, S.; Galla, H. J.; Janshoff, A. *Biophys. J.* **2000**, *79* (2), 904–918.

(35) Pathy, L. *J. Biol. Chem.* **1991**, *266* (10), 6035–6037.

(36) Hawgood, S.; Derrick, M.; Poulain, F. *Biochim. Biophys. Acta* **1998**, *1408* (2–3), 150–160.

(37) Andersson, M.; Curstedt, T.; Jornvall, H.; Johansson, J. *FEBS Lett.* **1995**, *362*, (3), 328–332.

(38) Pralle, A.; Keller, P.; Florin, E.-L.; Simons, K.; Horber, J. K. H. *J. Cell Biol.* **2000**, *148* (5), 997–1008.

(39) Simons, K.; Ehehalt, R. *J. Clin. Invest.* **2002**, *110* (5), 597–603.

(40) Vanderlick, T. K.; Moehwald, H. *J. Phys. Chem.* **1990**, *94*, 886–890.

(41) Heckl, W. M.; Cadenhead, D. A.; Moehwald, H. *Langmuir* **1988**, *4*, 1352–1358.

(42) Bailey, A. G.; Hashish, A. H.; Williams, T. J. *J. Electrostat.* **1998**, *44* (1–2), 3–10.

(43) Brand, P.; Friemel, I.; Meyer, T.; Schulz, H.; Heyder, J.; Haussinger, K. *J. Pharm. Sci.* **2000**, *89* (6), 724–731.

(44) Robertson, H. T.; Altmeier, W. A.; Glenn, R. W. *Ann. Biomed. Eng.* **2000**, *28* (8), 1028–1031.

(45) Tsuda, A.; Rogers, R. A.; Hydon, P. E.; Butler, J. P. *Proc. Natl. Acad. Sci. U.S.A.* **2002**, *99* (15), 10173–10178.

current study, the electrically different domains act as poles and give rise to an electrical field in the air above the interfacial film. Local field strength depends on both the lateral distribution and the potential difference between the local electrical poles. Therefore, the interaction of airborne particles with the lung's walls needs to be reevaluated, taking the electrostatic interaction with the surfactant film into account.

Acknowledgment. The current work was supported by the Canadian Institute for Health Research and the Canadian Foundation for Innovation. We thank Dr. Elmar Prenner for giving us access to a Langmuir trough and Dr. Robert French for careful correction of the manuscript.

LA061718G